Adipose tissue dysfunction and visceral fat are associated to hepatic insulin resistance and severity of NASH even in lean individuals

[1,#,$] *Chiara Saponaro, [1,#]Silvia Sabatini, [1]Melania Gaggini, [1]Fabrizia Carli, [2]Chiara Rosso, [3]Vincenzo Positano, [2]Angelo Armandi, [2]Gian Paolo Caviglia, [2]Riccardo Faletti, [2]Elisabetta Bugianesi, [1,*]Amalia Gastaldelli.

[1]Cardiometabolic Risk Unit, Institute of Clinical Physiology, CNR, Pisa, Italy.
[2]Division of Gastroenterology and Hepatology and Lab. of Diabetology, Dept. of Medical Sciences, University of Turin, Turin, Italy.
[3]Fondazione Toscana Gabriele Monasterio, Pisa, Italy.
[#]These authors contributed equally
[$]Current affiliation: Univ. Lille, CHU Lille, Inserm U1190, EGID, Lille, France.

***Correspondence to:**
Amalia Gastaldelli, PhD,
Head of Cardiometabolic Risk Unit
Institute of Clinical Physiology, CNR
via Moruzzi 1 56100 Pisa Italy
tel: +39 050 3152679/80
fax: +39 050 3152166
email: amalia@ifc.cnr.it

Chiara Saponaro, PhD
University of Lille, CHU Lille, Inserm U1190, EGID
Faculté de Médecine de Lille, Pôle Recherche
1, Place de Verdun
59045 - Lille, France
email: chiara.saponaro@univ-lille.fr

Number of words: 4011
Number of Tables: 1
Number of Figures: 4
Number of Supplementary Tables: 1
Number of Supplementary Figures: 2

Data availability statement

The data that support the findings of this study are available on request from the corresponding author. The data are not publicly available due to privacy or ethical restrictions.

Abbreviations

Nonalcoholic fatty liver disease (NAFLD)**,** Intrahepatic triglyceride (IHTG)**,** Subcutaneous fat (SC-AT)**,** Visceral fat (VF)**,** Free fatty acids (FFAs)**,** Triglyceride (TAG)**,** Non-alcoholic steatohepatitis (NASH)**,** NAFLD activity score (NAS), Hepatic insulin-resistance (Hep-IR), Muscle insulin-resistance (Muscle-IR), Adipose tissue insulin-resistance (Adipo-IR and Lipo-IR).

Conflict of Interest statement/Financial Disclosure

The authors declare no conflict of interest for this manuscript.

Acknowledgments and Funding: A.G. and E. B. received financial support from the European Union's Horizon 2020 for the project EpoS: Elucidating Pathways of Steatohepatitis (Grant agreement ID: 634413). A.G. received financial support from the European Union's Horizon 2020 Research and Innovation Programme under the Marie Skłodowska-Curie Grant Agreement ID 722619 (FOIE GRAS project) and Grant Agreement ID 734719 (mtFOIE GRAS project).

Lay summary

In this study we looked into the relationship between visceral vs. abdominal subcutaneous fat accumulation and the severity of NAFLD/NASH in lean, overweight, and obese individuals without diabetes compared to lean no-NAFLD. In comparison to no-NAFLD, severity of liver disease was related, independently of BMI, to greater visceral fat deposits that increased with the progression of the disease. In NAFLD/NASH visceral fat accumulation was linked also to insulin resistance in the liver, muscle, and adipose tissue, increased lipolysis, and lower adiponectin levels. Collectively, our findings imply that visceral fat buildup is a significant risk factor for severe NAFLD/NASH and may serve as an early signal of progression of this disease. Based on these findings, evidence-based preventive and management measures should be taken to target abdominal fat.

Abstract

Background & Aims: Nonalcoholic fatty liver disease (NAFLD) is a heterogeneous disorder, but the factors that determine this heterogeneity remain poorly understood. Adipose tissue dysfunction is causally linked to NAFLD since it causes intrahepatic triglyceride (IHTG) accumulation through increased hepatic lipid flow, due to insulin resistance and pro-inflammatory adipokines release. While many studies in NAFLD have looked at total adiposity (that is mainly subcutaneous fat, SC-AT), it is still unclear the possible impact of visceral fat (VF). Thus, we investigated how VF vs. SC-AT was related to NAFLD severity in lean, overweight, and obese individuals vs. lean controls.
Methods: Thirty-two non-diabetic NAFLD with liver biopsy (BMI 21.4 – 34.7 kg/m^2) and eight lean individuals (BMI 19.6 - 22.8 kg/m^2) were characterized for fat distribution (VF, SC-AT and IHTG by magnetic resonance imaging), lipolysis and insulin resistance by tracer infusion, free fatty acids (FFAs) and triglyceride (TAG) concentration and composition (by mass spectrometry).
Results: IHTG was positively associated with lipolysis, adipose tissue insulin resistance (Adipo-IR), TAG concentrations, and increased saturated/unsaturated FFA ratio. Compared to controls VF was higher in NAFLD (including lean individuals), increased with fibrosis stage and associated with insulin resistance in liver, muscle and adipose tissue, increased lipolysis, and decreased adiponectin levels. Collectively, our results suggest that VF accumulation, given its location close to the liver, is one of the major risk factors for NAFLD.
Conclusions: These findings propose VF as an early indicator of NAFLD progression independently of BMI, which may allow for evidence-based prevention and intervention strategies.
Keywords: NAFLD, fat distribution, visceral fat, subcutaneous fat, insulin resistance

Introduction

Non-alcoholic fatty liver disease (NAFLD) is a highly heterogeneous metabolic disorder covering a wide spectrum of liver diseases that ranges from simple steatosis to progressive inflammation, fibrosis, and ballooning, resulting in non-alcoholic steatohepatitis (NASH) and cirrhosis (1). The pathophysiology of the onset and progression of NAFLD is complex and is still not completely understood although it is established that NAFLD is a metabolic disease. In the last decades, a "multiple parallel hits hypothesis" has been proposed, in which not only excess calories and dietary components such as the westernized diet favor hepatic triglyceride accumulation and de novo fatty acid synthesis, but also the interactions between the liver and adipose tissue, together with the gut, play a concomitant role in the development of the disease.

Although the VF depot is much smaller than the SC-AT it provides a foreground effect, by driving the release of FFAs directly into the portal circulation (2, 3), possibly due to its enhanced lipolytic activity compared to that of SC-AT (4). Indeed, the accumulation of lipids in the VF is often complemented with storage in other ectopic sites, such as the liver and the pancreas (5). Moreover, hepatic and circulating lipid composition may also affect the extent of liver damage, inflammation, and the rate of disease progression (6, 7). Finally, in this complex scenario, hepatic and peripheral (muscle and adipose tissue) insulin resistance are central, although a causal link between steatosis, VF accumulation and insulin resistance requires more investigation. Although various *in vivo*, ex-situ and *in vitro* models have been extensively used to study the role of VF and insulin resistance in NAFLD (8-11), these models don't represent the full spectrum of human NAFLD progression (12). By contrast, numerous human studies, despite their translational value, are highly heterogeneous, due to ethnicity, sex, age, and the presence of confounding factors such as concomitant metabolic diseases, with and without drug treatment. Moreover, these studies are often confronted with limiting factors in the methodology such as the accurate measurement of parameters including fat distribution and insulin resistance. Therefore, the use of stable-isotope methodology provides a more thorough mechanistic readout of lipid metabolism and insulin resistance (13). Collectively, these techniques combined with the diagnosis and staging of NAFLD by non-invasive imaging techniques (14), will unveil whether or not VF accumulation and dysfunction are the initiators of NAFLD onset and progression. Upon recruitment of a cohort of non-diabetic Italian patients with various stages of NAFLD, stratified for BMI, we set out to determine the interplay of VF and insulin resistance at different stages of NAFLD. Indeed, we forecasted that this subset of patients would offer a unique setting to assess the direct impact of fat distribution and dysfunction on hepatic insulin resistance and steatosis, independently of diabetes, an area that has not been adequately investigated.

Materials and Methods

Patients. Thirty-two non-diabetic subjects, with biopsy-proven NAFLD and eight controls were enrolled for the study

that was part of the activities of the EU-FLIP project. Liver biopsies were scored according to Kleiner et al (15), altered fat topography, liver and pancreatic fat amount were measured by magnetic resonance imaging. The study was approved by the ethics committee of the University Hospital San Giovanni Battista of Torino and was in accordance with the Helsinki Declaration. All subjects signed an informed consent form before participating to the study.

***Liver damage and fibrosis score*.** Liver biopsy was scored according to Kleiner et al (15). The sum of grading for steatosis, lobular inflammation and hepatocellular ballooning was used to calculate the NAFLD activity score (NAS) from 0 to 8. Fibrosis was staged 0 to 4 and classified as absent (0), mild (1-2) and severe (3-4). NASH was defined by the local pathologist according to the joint presence of steatosis, hepatocyte ballooning and lobular inflammation with or without fibrosis.

Fat topography by magnetic resonance imaging. Hepatic fat quantification was assessed by Hepatic Magnetic Resonance Imaging Proton Density Fat Fraction (MRI-PDFF). Magnetic resonance images were acquired using the DIXON method following protocols previously published (16). For each slice the subcutaneous abdominal fat area was measured by automatic detection of the outer and inner margins of subcutaneous adipose tissue as region of interest (ROI) from the cross-sectional images, and by counting the number of pixels between the outer and inner margins of subcutaneous adipose tissue; volume was automatically calculated by multiplying the slice area by the slice thickness and then the values of all slices were summed to obtain the abdominal fat volume. For each slice visceral (intra-abdominal) fat area and volume was determined with the use of histograms specific to the visceral region and then summed to obtain the abdominal VF volume. A factor of 0.92 was used to convert adipose tissue volume into adipose tissue mass (17). To quantify liver fat fraction (IHTG) the reconstructed fat and water image were analyzed using the OsiriX program (18); 3 regions of interest (ROI) (30 × 30 mm) were quantified in the reconstructed fat and water images. Fat content was calculated from signal intensity in the ROIs of the in-phase (IP) and opposed-phase (OP) images as [(IP-OP)/(2 x OP) × 100] (16, 19). Hepatic fat content was considered normal if < 5.6% (20).

***Plasma measurements*.** In all subjects we measured fasting plasma lipid profile, concentrations of FFA, triglycerides, total cholesterol, high-density lipoprotein (HDL), low-density lipoprotein (LDL), Liver function tests, apolipoprotein B (APO-B), apolipoprotein A1 (APO-A1), glucose, insulin and C-peptide, as previously reported (21). Circulating adiponectin was measured by an ELISA Milliplex Assay (Merck KGaA, Darmstadt, Germany).

Metabolic indexes. Endogenous glucose production (µmol/min Kg_FFM) and peripheral glucose clearance (ml/min Kg FFM) were measured by the kinetics of 6,6-D2-glucose infused for 2 hours during a fasting state, following a protocol previously reported (22).

Hepatic insulin resistance (Hep-IR) reflects the inability of insulin to suppress fasting endogenous glucose production (EGP) and was calculated as the product of EGP x fasting insulin (21) while Muscle-IR was measured as the inverse of peripheral glucose clearance normalized by fasting insulin (22).
Lipolysis (µmol/min) was measured by the kinetics of D5-glycerol infused for 2 hours during a fasting state, following a protocol previously reported (22). Adipose tissue insulin resistance reflects the inability of insulin to exert an antilipolytic action, leading to a relative increase in lipolysis and fasting FFA concentrations (23). Lipo-IR was calculated as the product of fasting lipolysis x insulin while Adipo-IR was calculated as the product of fasting FFA x insulin (23).

***Metabolite analysis*.** Free fatty acid composition was evaluated by GC-MS (Agilent technology GC7890-MS5975). Briefly, separation of lipid fraction from 20uL of plasma was carried out with a methanol and chloroform (2:1) solution using the Folch's method (24). Fatty acids were derivatized to methyl-ester with a solution of methanol-BF3 14% and dried. Samples were reconstituted with 70 µL heptane and 1 µL was injected in the GC-MS. Total plasma FFA concentration was measured spectrophotometric ally on Beckman analyzer (Waco, Global Medical Instrumentation, Ramsey, MN). Single fatty acid concentration was determined using as internal standard a mix of 13C labeled FFA (Alga mix, CIL Cambridge MA, USA) and heptadecanoic acid. We quantified saturated (SFA, myristic, palmitic and stearic acid), and unsaturated (UFA, i.e., the mono-unsaturated oleic and palmitoleic acids and the poly-unsaturated linoleic and arachidonic acids) fatty acid concentrations. The ratio of SFA/UFA was calculated as parameter of lipotoxicity. Triglycerides (TAGs) plasma composition was analyzed by ultra-high-pressure liquid chromatography/quadrupole time-of-flight mass spectrometry (UHPLC/Q-TOF, 1290 Infinity-6540 Agilent Technology, Santa Clara, CA) equipped with electrospray ionization (ESI). Plasma (20µL) was deproteinized with 200µL of cold methanol (Merck, Darmstadt, Germany), centrifuged at 14000 rpm for 20 minutes and the supernatant was transferred into glass vials and 1 µL was injected into the LC/MS. Triglycerides were separated used an Agilent ZORBAX Eclipse Plus C18 2.1 × 100 mm 1.8-Micron and acquisition was set in positive mode. TG species were analyzed using Agilent MassHunter Profinder B.06.00. Analysis of TG composition was qualitative: area of each specie was normalized to total area of triglycerides. TGs were classified as low unsaturated by calculating sum of areas of TGs with 0 and 1 double bonds (0-1 db) and unsaturated by calculating sum of areas of TGs with 2- 5 double bonds (2-5 db).

Statistical analysis. Variables were expressed as mean +/- standard error (SE). Differences in distribution among groups were calculated using non parametric Mann-Whitney's test. Quade's test was used to perform a non-parametric rank analysis of covariance (ANCOVA) (25). Correlation analysis was performed using Pearson's

correlation coefficient, after a log transformation of variables.

Heatmaps were created reporting data as median within the groups of interest. Data were therefore centered and scaled in the row direction to improve interpretability. All statistical analysis was performed using R Statistical Software (version 4.0.5).

Results

1. Clinical characteristics of study subjects

We studied thirty-two subjects with biopsy-proven NAFLD (20 NASH and 12 NAFL) with a wide range of BMI (*n* = 10 with BMI <25; *n* = 12 with BMI ≥ 25 and <30; *n* = *12* with BMI ≥30) and eight lean controls (**Fig. 1A**). Controls were statistically younger compared to NAFLD individuals, although there was no statistical difference among subjects with NAFLD. After adjustment for BMI and age, fasting glycemia, circulating FFAs and HDL were not significantly different among the 4 groups (**Table 1**). Plasma levels of liver enzymes were significantly higher in NAFLD compared to the control group, i.e., alanine aminotransferase (ALT: 75.0 ± 6.4 vs 16.3 ± 1.6 U/l), aspartate aminotransferase (AST: 45.7 ± 6.2 vs 19.6 ± 1.6 U/l) and gamma-glutamyltransferase (GGT: 105.9 ± 21.2 vs 14.3 ± 4.2 U/l, all p<0.0002). Total TG, LDL and cholesterol were higher in NAFLD subjects compared to the controls (**Table 1**).

2. Obesity and adipose tissue distribution in NAFLD

Subjects with NAFLD were divided into 3 groups according to their BMI as lean (BMI <25 kg/m^2), overweight (BMI ≥ 25 and <30 kg/m^2) and obese (BMI ≥ 30 kg/m^2). BMI of lean individuals with NAFLD was similar to healthy lean subjects without NAFLD (23.2 ± 0.6 vs 21.2 ± 0.6 kg/m^2) (**Fig. 1A**). Excessive intrahepatic triglyceride content (IHTG) (**Fig. 1B**) and visceral fat (VF) (**Fig. 1D**) measured by MRI-PDFF were increased in all NAFLD compared to the lean controls. SC-AT, on the other hand, was significantly increased only in overweight and obese NAFLD, compared to the lean NAFLD and lean controls (**Fig. 1C**). Obesity (BMI≥30 kg/m^2) was associated to a further increase in all fat depots (**Fig. 1B-D**). A strong positive correlation was observed between IHTG obtained by MRI-PDFF and the measurement of steatosis assessed by the pathologist on liver biopsy (r=0.74, p<0001; **Supplementary Fig. 1**).

We analyzed body fat distribution according to the grade of steatosis, lobular inflammation and hepatocellular ballooning (NAS score, two groups NAS≤3 and NAS≥4) (**Fig. 2 A-D**). In our cohort there were no patients with NAS score greater than 6. As expected, hepatic fat increased proportionally with the grade of NAS score, while BMI, VF and SC-AT showed a trend to be higher in NAFLD patients with high NAS score without reaching statistical significance (**Fig. 2 A-D**).

In the analysis of body fat distribution according to the degree of fibrosis (**Fig. 3 A-D**) we observed that subjects with severe fibrosis (i.e. F2-F4), had higher BMI, SC-AT and VF compared to F01 and to lean controls (**Fig. 3 A,C,D**), in line with previous studies (26). Furthermore, in this cohort IHTG, VF and SC-AT were not associated to necroinflammation, defined by inflammation plus ballooning (**Supplementary Fig. 2A-D**), thus

suggesting that the IHTG, VF and SC-AT are mainly associated to steatosis (**Fig 2A-D**) and fibrosis (**Fig. 3A-D**) progression and less to necroinflammation stage.

3. Insulin resistance and adipose tissue distribution in NAFLD

Tracer infusion allowed the measurement of metabolic fluxes such as adipose tissue lipolysis and endogenous glucose production (mainly hepatic), and to evaluate insulin resistance in the liver (Hep-IR), muscle (Muscle-IR) and adipose tissue (as Adipo-IR and Lipo-IR). Given that control subjects were younger compared to NAFLD individuals, analysis was corrected by age. Adipose tissue lipolysis was increased in NAFLD compared to healthy controls (p=0.006, adjusted for age), especially in those with NAS 4-6 and fibrosis F2-4 (**Fig. 2E** and **3E**) and associated not only with BMI, but also with increased abdominal fat VF, SC-AT and IHTG (**Fig. 1E**). Moreover, lipolysis was positively correlated with increased FFA concentrations demonstrating the increased overflow of fatty acids from the periphery to other organs in subjects with NAFLD (**Fig. 1E**). The associations were similar in NAFL and NASH (data not shown), but lipolysis was higher in subjects with more severe forms of NAFLD, i.e., in subjects with NAS ≥4 (**Fig. 2E**) and with fibrosis ≥2 (**Fig. 3E**). Adipose tissue IR that measures the defective action of insulin in suppressing peripheral lipolysis (here measured as Adipo-IR and Lipo-IR) was positively associated with IHTG (**Fig. 1E**) and was higher in NAFLD subjects with a more severe liver disease (**Fig. 2E and 3E**). Of note, VF was also inversely associated with circulating adiponectin levels (**Fig.1E**), the most abundant anti-inflammatory and atheroprotective adipokine secreted by adipose tissues (27) that is also a marker of insulin sensitivity. However, we did not observe a correlation between SC-AT and adiponectin levels, in line with previous studies (28, 29). Moreover, we found that adiponectin was significantly decreased in all NAFLD individuals compared to controls also in those with low BMI ($p < 0.02$), and it was inversely correlated with Hep-IR (rho= -0.50, $p<0.001$), and IHTG accumulation (**Fig. 1E**), thus posing the possibility of an additional mechanism by which VF negatively impacts liver function and promotes NAFLD. Endogenous glucose production was slightly higher in subjects NAFLD compared to lean controls (14.2±0.3 vs 11.7±0.6 µmol/min per Kg of fat free mass, p=0.001) including in lean NAFLD (p=0.02). Hep-IR and Muscle-IR were increased in NAFLD subjects, especially in those with a more severe liver disease, i.e., in subjects with NAS ≥4 (**Fig. 2E**) and with fibrosis ≥2 (**Fig. 3E**). VF and SC-AT were strongly correlated with Hep-IR, and with a less extent to Muscle-IR (**Fig. 1E**).

Higher fibrosis stage was associated to higher SFA/UFA ratio, palmitic/linoleic acid ratio (DNL index), insulin, endogenous glucose production, HOMA, adipo-IR and hepatic, but not muscle, insulin resistance (**Fig. 3E**), even after adjusting for IHTG (**Supplementary Table 1**).

4. Lipid concentrations and composition, and adipose tissue distribution in NAFLD

Although BMI was associated to increased lipid concentrations, only VF and IHTG, not SC-AT, were associated to increased circulating TG and ApoB concentrations (**Fig. 1E**) indicating increased synthesis and secretion of VLDL, likely stimulated by a high portal lipid supply given that VF is more lipolytic than SC-AT (30).

The analysis of FFA and TG composition showed a shift towards increased saturated FFAs and TGs in NAFLD vs controls, although the increase was more pronounced in subjects with BMI≥30 (**Fig. 4 A,C**). The severity of liver disease (i.e., higher fibrosis) was associated to higher circulating saturated fatty acids both as FFA (**Fig. 4 B**), such as myristic, palmitic and stearic acid, with a depletion of linoleic acid, as well as higher saturated TG (**Fig. 4 D**).

We also observed that the saturated/unsaturated fatty acid ratio (in TAG and FFA) was associated to increased Adipo-IR, Hep-IR, Muscle-IR and IHTG accumulation, and to a lesser extent to SC-AT but not to VF (**Fig. 4 E**), likely because the fatty acids released by VF into the portal vein are in great part taken up by the liver.

Discussion

Abdominal obesity is a known risk factor for the development of NAFLD (26) since it is strictly related to peripheral and hepatic insulin resistance (31). The rate of FFA mobilization from the adipocytes embedded within the deep abdominal adipose tissue is higher compared to SC-AT (4, 32, 33), and previous studies suggested that VF is more strongly related to insulin resistance than SC-AT (34). The impaired antilipolytic effect of insulin on adipose tissue and the FFA efflux from the VF directly to the liver through the preferential portal vein, affects liver function, thus promoting steatosis. But whether VF accumulation is the cause or the consequence of the onset and development of NAFLD is still being debated. In this study, we corroborate a strong correlation between VF accumulation and Hep-IR and IHTG accumulation, which occur also in lean NAFLD individuals without diabetes.

Although several studies demonstrated the involvement of VF in insulin resistance especially in the liver (21, 35-37), there are conflicting data in this regard. We have shown that fasting endogenous glucose production and gluconeogenesis were associated only to increased VF while Hep-IR and impaired insulin mediated suppression endogenous glucose production were associated to both VF and IHTG (21). Fabbrini et al. questioned the role of VF, compared to IHTG, in the association with insulin resistance (38); however, the group matched for IHTG with high/low VF had a mean hepatic fat of 13.3% (38), i.e. double the limit for NAFLD. A reanalysis of the data by grouping the subjects from low IHTG-Low VF to high IHTG-high VF showed that insulin resistance is increased proportionally with both visceral and liver fat (31). The importance of high VF regardless of high or low IHTG was also confirmed in a recent study that showed how VF was associated to higher risk of type 2 diabetes (39). The preferential accumulation of fat and calories in visceral rather than subcutaneous fat, can be related to adipose tissue expansion, either by a combination of an increase in adipocyte number (hyperplasia), or size (hypertrophy). While hyperplasia is

associated with a beneficial and protective asset of adipose tissue, hypertrophy results in increased inflammation, macrophage infiltration, and reduced insulin sensitivity (40). Whether VF is more prone to expand in a hypertrophic manner and develop inflammation compared to SC-AT is still unclear. It has been proposed that VF and IHTG accumulation are the consequence of a dysfunctional SC-AT that limits peripheral adipose tissue expansion. Treatment with pioglitazone ameliorates adipose tissue dysfunction and determines fat redistribution by decreasing both VF and IHTG and increasing SC-AT (41, 42). Lipodystrophy is often study as a model of dysfunctional adipose tissue since it is associated with low subcutaneous fat and hepatic fat accumulation. Patients with generalized lipodystrophy have also low VF, while those with partial lipodystrophy have high VF (43). Patients with severe lipodystrophy have also increased lipolysis and severe Hep-IR (44). We have recently shown that the reduction of hepatic fat after pioglitazone treatment and the improvement in liver histology, was mediated by the decrease in VF and increase in SC-AT (ie by the VF/SC-AT ratio) (42). These results indicate that the excess FFA that is not stored in the subcutaneous adipose tissue is then metabolized in the liver, thus increasing hepatic TG accumulation.

It has been reported that lean NAFLD individuals had a higher amount of daily calory intake compared to lean controls (45, 46). Notably, the Diabetes Remission Clinical Trial (DiRECT) study recently revealed a significant and sustained improvement of T2D remission and β-cell function after a very low-calorie diet in patients with early onset of the disease. Calorie restriction produced a substantial weight-loss, which was associated with a decrease in hepatic and intra-pancreatic fat content (47, 48). Therefore, reducing calory intake may be an efficient strategy to reduce VF accumulation, thus avoiding the deleterious consequences that triggers the onset of Hep-IR and steatosis. The reason why an accumulation of VF occurs independent of weight-gain is not so clear. Some studies suggest that it may be related to stress associated with overeating or increased cortisol clearance. Genetics may also accentuate VF accumulation in response to stress (49). Moreover, the characteristics of the subcutaneous adipose tissue and the expression of lipid storage-related genes determines the expansion of subcutaneous adipose tissue in response to excessive caloric intake (50).

Adipose tissue is not only a reservoir for energy storage and utilization, but also senses energy demands and secrete adipokines such as adiponectin, which exerts protective actions for liver injury by enhancing fatty acid β-oxidation, and reducing Hep-IR (51, 52). Moreover, it has been already established that adiponectin reduces hepatic gluconeogenesis and increases glucose uptake and whole-body insulin sensitivity (53, 54). Studies on the association of adiponectin with VF rather than SC-AT have been conflicting (55-57). Here, we showed that adiponectin levels were reduced in response to increased VF, and were inversely associated with increased Hep-IR, and steatosis. A significant decrease of circulating

adiponectin was observed in lean NAFLD individuals compared to controls, thus suggesting that circulating levels of adiponectin as a potential biomarker to track development of NAFLD, VF accumulation and dysfunction. Thus, fat distribution is an important risk factor for the development and progression of NAFLD, because VF, unlike SC-AT, not only contributes to hepatic fatty acid overflow but it is significantly increased in the early stages of the disease.

Not only excessive caloric intake but also excess intake of saturated fat can be crucial in driving VF accumulation and liver damage (58) and also being associated to more severe forms of NAFLD (59). It is already known that different classes of lipids, according to their degree of saturation, can impact metabolism. An increased proportion of unsaturated compared to saturated fatty acids, i.e., a decreased SFA/UFA ratio in animal models, has been associated, with a favorable serum lipid profile and activation of hepatic enzymes involved in antioxidative pathways (60). A diet high in UFA and low in SFA decreases fat accumulation in white adipose tissue, and is associated with increased expression of hepatic lipolytic enzymes and enhanced fatty acid β-oxidation (61). Previous studies have shown that subjects with NAFLD have higher intrahepatic and circulating lipids containing saturated fatty acids (59, 62). In line with these results, target lipidomic analysis performed here revealed that novel lipid species may serve as early markers of liver damage such as SFA and saturated TG, independently of obesity. We also hypothesized that the SFA/UFA ratio, in either circulating free fatty acids or TGs, could be considered as an index for the evaluation of metabolic health. Our results show that in NAFLD individuals the SFA/UFA ratio was significantly increased compared to healthy subjects especially in those with high fibrosis stage, indicating an imbalance in SFA in NAFLD, as previously suggested (62-64). These lipid alterations were strongly correlated with increased VF, Adipo-IR, Hep-IR and IHTG. These metabolic disturbances result in an increased demand for insulin secretion to 'overcome' insulin resistance, thus setting in place a vicious cycle. Indeed, insulin resistance is tethered to higher levels of insulin than expected relative to the level of glucose.

Although the results of this study are confirmatory, the main strength of our study is that we investigated non diabetic individuals with biopsy-proven NAFLD, i.e., excluding confounding factors strongly related to visceral adiposity, such diabetes and antidiabetic treatments, which influence fat accumulation and distribution (65, 66). Moreover, the individuals BMI ranged from 18-37 kg/m^2 which allowed us to stratify individuals by BMI and explore the pivotal role of VF on IHTG accumulation and damage, independently of body weight. Furthermore, the use of tracer studies provided a more thorough understanding of the association of VF with lipid and glucose fluxes, and IR in liver muscle and adipose tissue.

A limitation of the study is the low number of patients recruited to a single center, but this was due to difficulties and costs to perform tracer studies and MRI scans in a large number of subjects. In addition, we did not perform analysis stratified by sex, because the women recruited in this

study were less than men. Therefore, we cannot ignore that sex differences can influence VF and SC-AT distribution, and correlation with hepatic fat content (32). Future studies on larger cohorts stratified for sex and BMI would be beneficial to study the onset and progression of lean NAFLD.

In conclusion, our findings suggest elevated VF accumulation and saturated lipids as early indicators of severe NAFLD regardless of BMI, therefore insinuating fat composition and distribution as key players in the regulation of lipid metabolism and NAFLD progression. A deeper investigation of fat distribution would be instrumental in defining the best targeted-interventional approach and to characterize patients at increased risk of disease development.

References

1. Petta S, Gastaldelli A, Rebelos E, et al. Pathophysiology of Non Alcoholic Fatty Liver Disease. Int J Mol Sci 2016; 17(12).
2. Saponaro C, Gaggini M, Carli F, Gastaldelli A. The Subtle Balance between Lipolysis and Lipogenesis: A Critical Point in Metabolic Homeostasis. Nutrients 2015; 7(11): 9453-74.
3. Yki-Jarvinen H. Non-alcoholic fatty liver disease as a cause and a consequence of metabolic syndrome. Lancet Diabetes Endocrinol 2014; 2(11): 901-10.
4. Zierath J R, Livingston J N, Thorne A, et al. Regional difference in insulin inhibition of non-esterified fatty acid release from human adipocytes: relation to insulin receptor phosphorylation and intracellular signalling through the insulin receptor substrate-1 pathway. Diabetologia 1998; 41(11): 1343-54.
5. Singh R G, Yoon H D, Wu L M, Lu J, Plank L D, Petrov M S. Ectopic fat accumulation in the pancreas and its clinical relevance: A systematic review, meta-analysis, and meta-regression. Metabolism 2017; 69: 1-13.
6. Dongiovanni P, Stender S, Pietrelli A, et al. Causal relationship of hepatic fat with liver damage and insulin resistance in nonalcoholic fatty liver. Journal of internal medicine 2018; 283(4): 356-70.
7. Lytle K A, Bush N C, Triay J M, et al. Hepatic Fatty Acid Balance and Hepatic Fat Content in Humans With Severe Obesity. J Clin Endocrinol Metab 2019; 104(12): 6171-81.
8. Akagiri S, Naito Y, Ichikawa H, et al. A Mouse Model of Metabolic Syndrome; Increase in Visceral Adipose Tissue Precedes the Development of Fatty Liver and Insulin Resistance in High-Fat Diet-Fed Male KK/Ta Mice. J Clin Biochem Nutr 2008; 42(2): 150-7.
9. Franczyk M P, He M, Yoshino J. Removal of Epididymal Visceral Adipose Tissue Prevents Obesity-Induced Multi-organ Insulin Resistance in Male Mice. J Endocr Soc 2021; 5(5): bvab024.
10. Jones P H, Deng B, Winkler J, et al. Over-expression of miR-34c leads to early-life visceral fat accumulation and insulin resistance. Sci Rep 2019; 9(1): 13844.
11. Yang J, Park K W, Cho S. Inhibition of the CD36 receptor reduces visceral fat accumulation and improves insulin resistance in obese mice carrying the BDNF-Val66Met variant. J Biol Chem 2018; 293(34): 13338-48.

12. Green C J, Parry S A, Gunn P J, et al. Studying non-alcoholic fatty liver disease: the ins and outs of in vivo, ex vivo and in vitro human models. Horm Mol Biol Clin Investig 2018; 41(1).
13. McCullough A, Previs S, Kasumov T. Stable isotope-based flux studies in nonalcoholic fatty liver disease. Pharmacol Ther 2018; 181: 22-33.
14. Miele L, Zocco M A, Pizzolante F, et al. Use of imaging techniques for non-invasive assessment in the diagnosis and staging of non-alcoholic fatty liver disease. Metabolism 2020; 112: 154355.
15. Kleiner D E, Brunt E M, Van Natta M, et al. Design and validation of a histological scoring system for nonalcoholic fatty liver disease. Hepatology 2005; 41(6): 1313-21.
16. Ishizaka K, Oyama N, Mito S, et al. Comparison of 1H MR spectroscopy, 3-point DIXON, and multi-echo gradient echo for measuring hepatic fat fraction. Magn Reson Med Sci 2011; 10(1): 41-8.
17. Sironi A M, Gastaldelli A, Mari A, et al. Visceral fat in hypertension: influence on insulin resistance and beta-cell function. Hypertension 2004; 44(2): 127-33.
18. Rosset A, Spadola L, Ratib O. OsiriX: an open-source software for navigating in multidimensional DICOM images. J Digit Imaging 2004; 17(3): 205-16.
19. Tang A, Desai A, Hamilton G, et al. Accuracy of MR imaging-estimated proton density fat fraction for classification of dichotomized histologic steatosis grades in nonalcoholic fatty liver disease. Radiology 2015; 274(2): 416-25.
20. Szczepaniak L S, Nurenberg P, Leonard D, et al. Magnetic resonance spectroscopy to measure hepatic triglyceride content: prevalence of hepatic steatosis in the general population. Am J Physiol Endocrinol Metab 2005; 288(2): E462-8.
21. Gastaldelli A, Cusi K, Pettiti M, et al. Relationship between hepatic/visceral fat and hepatic insulin resistance in nondiabetic and type 2 diabetic subjects. Gastroenterology 2007; 133(2): 496-506.
22. Camastra S, Astiarraga B, Tura A, et al. Effect of exenatide on postprandial glucose fluxes, lipolysis, and ss-cell function in non-diabetic, morbidly obese patients. Diabetes Obes Metab 2017; 19(3): 412-20.
23. Gastaldelli A, Gaggini M, DeFronzo R A. Role of adipose tissue insulin resistance in the natural history of type 2 diabetes: results from the San Antonio Metabolism Study. Diabetes 2017; 66(4): 815-22.
24. Folch J, Lees M, Sloane Stanley G H. A simple method for the isolation and purification of total lipides from animal tissues. J Biol Chem 1957; 226(1): 497-509.
25. Quade D. Rank Analysis of Covariance. Journal of the American Statistical Association 1967; 62(320): 1187-200.
26. van der Poorten D, Milner K L, Hui J, et al. Visceral fat: a key mediator of steatohepatitis in metabolic liver disease. Hepatology 2008; 48(2): 449-57.
27. Esfahani M, Movahedian A, Baranchi M, Goodarzi M T. Adiponectin: an adipokine with protective features against metabolic syndrome. Iran J Basic Med Sci 2015; 18(5): 430-42.
28. Konigorski S, Janke J, Drogan D, et al. Prediction of Circulating Adipokine Levels Based on Body Fat Compartments and Adipose Tissue

Gene Expression. Obes Facts 2019; 12(6): 590-605.
29. Gastaldelli A, Sironi A M, Ciociaro D, et al. Visceral fat and beta cell function in non-diabetic humans. Diabetologia 2005; 48(10): 2090-6.
30. Riches F M, Watts G F, Hua J, Stewart G R, Naoumova R P, Barrett P H. Reduction in visceral adipose tissue is associated with improvement in apolipoprotein B-100 metabolism in obese men. J Clin Endocrinol Metab 1999; 84(8): 2854-61.
31. Gaggini M, Morelli M, Buzzigoli E, DeFronzo R A, Bugianesi E, Gastaldelli A. Non-alcoholic fatty liver disease (NAFLD) and its connection with insulin resistance, dyslipidemia, atherosclerosis and coronary heart disease. Nutrients 2013; 5(5): 1544-60.
32. Brand T, van den Munckhof I C L, van der Graaf M, et al. Superficial vs Deep Subcutaneous Adipose Tissue: Sex-Specific Associations With Hepatic Steatosis and Metabolic Traits. J Clin Endocrinol Metab 2021; 106(10): e3881-e89.
33. Monzon J R, Basile R, Heneghan S, Udupi V, Green A. Lipolysis in adipocytes isolated from deep and superficial subcutaneous adipose tissue. Obes Res 2002; 10(4): 266-9.
34. Liu L, Feng J, Zhang G, et al. Visceral adipose tissue is more strongly associated with insulin resistance than subcutaneous adipose tissue in Chinese subjects with pre-diabetes. Curr Med Res Opin 2018; 34(1): 123-29.
35. Krishnappa S K, Yashoda H T, Boraiah G, Vishwa S. Sagittal Abdominal Diameter to Measure Visceral Adipose Tissue in Overweight or Obese Adolescent Children and Its Role as A Marker of Insulin Resistance. J Clin Diagn Res 2015; 9(11): SC09-12.
36. Mendelson M, Michallet A S, Monneret D, et al. Impact of exercise training without caloric restriction on inflammation, insulin resistance and visceral fat mass in obese adolescents. Pediatr Obes 2015; 10(4): 311-9.
37. Preis S R, Massaro J M, Robins S J, et al. Abdominal subcutaneous and visceral adipose tissue and insulin resistance in the Framingham heart study. Obesity (Silver Spring) 2010; 18(11): 2191-8.
38. Fabbrini E, Magkos F, Mohammed B S, et al. Intrahepatic fat, not visceral fat, is linked with metabolic complications of obesity. Proceedings of the National Academy of Sciences of the United States of America 2009; 106(36): 15430-5.
39. Tejani S, McCoy C, Ayers C R, et al. Cardiometabolic Health Outcomes Associated With Discordant Visceral and Liver Fat Phenotypes: Insights From the Dallas Heart Study and UK Biobank. Mayo Clin Proc 2021.
40. Longo M, Zatterale F, Naderi J, et al. Adipose Tissue Dysfunction as Determinant of Obesity-Associated Metabolic Complications. Int J Mol Sci 2019; 20(9).
41. White U, Fitch M D, Beyl R A, Hellerstein M K, Ravussin E. Adipose depot-specific effects of 16 weeks of pioglitazone on in vivo adipogenesis in women with obesity: a randomised controlled trial. Diabetologia 2021; 64(1): 159-67.
42. Gastaldelli A, Sabatini S, Carli F, et al. PPAR-gamma-induced changes in visceral fat and adiponectin levels are associated with improvement of steatohepatitis in patients with NASH.

Liver international : official journal of the International Association for the Study of the Liver 2021; 41(11): 2659-70.
43. Polyzos S A, Perakakis N, Mantzoros C S. Fatty liver in lipodystrophy: A review with a focus on therapeutic perspectives of adiponectin and/or leptin replacement. Metabolism 2019; 96: 66-82.
44. Petersen K F, Oral E A, Dufour S, et al. Leptin reverses insulin resistance and hepatic steatosis in patients with severe lipodystrophy. J Clin Invest 2002; 109(10): 1345-50.
45. Albhaisi S, Chowdhury A, Sanyal A J. Non-alcoholic fatty liver disease in lean individuals. JHEP Rep 2019; 1(4): 329-41.
46. Sharp K P H, Schultz M, Coppell K J. Is non-alcoholic fatty liver disease a reflection of what we eat or simply how much we eat? JGH Open 2018; 2(2): 59-74.
47. Taylor R, Al-Mrabeh A, Zhyzhneuskaya S, et al. Remission of Human Type 2 Diabetes Requires Decrease in Liver and Pancreas Fat Content but Is Dependent upon Capacity for beta Cell Recovery. Cell Metab 2018; 28(4): 547-56 e3.
48. Taylor R, Leslie W S, Barnes A C, et al. Clinical and metabolic features of the randomised controlled Diabetes Remission Clinical Trial (DiRECT) cohort. Diabetologia 2018; 61(3): 589-98.
49. Drapeau V, Therrien F, Richard D, Tremblay A. Is visceral obesity a physiological adaptation to stress? Panminerva Med 2003; 45(3): 189-95.
50. Alligier M, Gabert L, Meugnier E, et al. Visceral fat accumulation during lipid overfeeding is related to subcutaneous adipose tissue characteristics in healthy men. J Clin Endocrinol Metab 2013; 98(2): 802-10.
51. Neumeier M, Weigert J, Schaffler A, et al. Aldehyde oxidase 1 is highly abundant in hepatic steatosis and is downregulated by adiponectin and fenofibric acid in hepatocytes in vitro. Biochem Biophys Res Commun 2006; 350(3): 731-5.
52. Xu A, Wang Y, Keshaw H, Xu L Y, Lam K S, Cooper G J. The fat-derived hormone adiponectin alleviates alcoholic and nonalcoholic fatty liver diseases in mice. J Clin Invest 2003; 112(1): 91-100.
53. Yamauchi T, Kamon J, Waki H, et al. The fat-derived hormone adiponectin reverses insulin resistance associated with both lipoatrophy and obesity. Nature medicine 2001; 7(8): 941-6.
54. Bugianesi E, Pagotto U, Manini R, et al. Plasma adiponectin in nonalcoholic fatty liver is related to hepatic insulin resistance and hepatic fat content, not to liver disease severity. J Clin Endocrinol Metab 2005; 90(6): 3498-504.
55. Cho S A, Joo H J, Cho J Y, et al. Visceral Fat Area and Serum Adiponectin Level Predict the Development of Metabolic Syndrome in a Community-Based Asymptomatic Population. PLoS One 2017; 12(1): e0169289.
56. Frederiksen L, Nielsen T L, Wraae K, et al. Subcutaneous rather than visceral adipose tissue is associated with adiponectin levels and insulin resistance in young men. J Clin Endocrinol Metab 2009; 94(10): 4010-5.
57. Gariballa S, Alkaabi J, Yasin J, Al Essa A. Total adiponectin in overweight and obese subjects and its response to visceral fat loss. BMC Endocr Disord 2019; 19(1): 55.
58. Luukkonen P K, Sadevirta S, Zhou Y, et al. Saturated Fat Is More

Metabolically Harmful for the Human Liver Than Unsaturated Fat or Simple Sugars. Diabetes Care 2018; 41(8): 1732-39.
59. Masoodi M, Gastaldelli A, Hyotylainen T, et al. Metabolomics and lipidomics in NAFLD: biomarkers and non-invasive diagnostic tests. Nature reviews Gastroenterology & hepatology 2021.
60. Kang M J, Shin M S, Park J N, Lee S S. The effects of polyunsaturated:saturated fatty acids ratios and peroxidisability index values of dietary fats on serum lipid profiles and hepatic enzyme activities in rats. Br J Nutr 2005; 94(4): 526-32.
61. Liao F H, Liou T H, Shieh M J, Chien Y W. Effects of different ratios of monounsaturated and polyunsaturated fatty acids to saturated fatty acids on regulating body fat deposition in hamsters. Nutrition 2010; 26(7-8): 811-7.
62. Roumans K H M, Lindeboom L, Veeraiah P, et al. Hepatic saturated fatty acid fraction is associated with de novo lipogenesis and hepatic insulin resistance. Nat Commun 2020; 11(1): 1891.
63. Hodson L, Rosqvist F, Parry S A. The influence of dietary fatty acids on liver fat content and metabolism. Proc Nutr Soc 2020; 79(1): 30-41.
64. Puri P, Baillie R A, Wiest M M, et al. A lipidomic analysis of nonalcoholic fatty liver disease. Hepatology 2007; 46(4): 1081-90.
65. Koshizaka M, Ishikawa K, Ishibashi R, et al. Comparison of Visceral Fat Reduction by Ipragliflozin and Metformin in Elderly Type 2 Diabetes Patients: Sub-Analysis of a Randomized-Controlled Study. Diabetes Ther 2021; 12(1): 183-96.
66. Shimabukuro M, Tanaka H, Shimabukuro T. Effects of telmisartan on fat distribution in individuals with the metabolic syndrome. J Hypertens 2007; 25(4): 841-8.

Table 1 Clinical characteristics of study subjects

	Control	**NAFLD**	**NAFLD**	**NAFLD**	**CT vs NAFLD**	
	BMI ≤25 (n=8)	BMI ≤25 (n=10)	BMI ≤30 (n=12)	BMI >30 (n=10)	p value adjusted for age	p value adjusted for age and BMI
Gender M/F	4/4	8/2	10/2	8/2	-	-
Age	26.9±1.7	39.3±8.6*	49.6±12.9*	36.7±11.7*	-	-
BMI (Kg/m^2)	21.2±1.6	23.2±1.8*	27.4±1.3*	32.5±2.2*	<0.0001	-
ALT (U/l)	16.3±4.4	57.7±19.8*	66.0±34.4*	98.5±41.2*	<0.0001	0.0008
AST (U/l)	19.6±4.4	35.8±16.8*	49.5±57.7*	50.1±14.0*	0.0005	0.0133
GGT (U/l)	14.3±11.9	155.1±110.3*	62.6±59.9*	108.3±165.8*	0.0008	0.0022
Glucose (mg/dL)	90.8±5.6	94.8±8.1	96.5±11.5	98.0±14.8	0.9954	0.7545
Insulin (mU/L)	5.9±1.8	8.9±2.8*	11.9±3.2*	12.4±8.7*	0.0008	0.0221
TG (mg/dL)	56.1±18.6	90.1±22.2*	107.5±60.6*	118.3±69.2*	0.0199	0.0882
FFA (mmol/L)	0.6±0.2	0.6±0.1	0.6±0.3	0.7±0.2	0.8372	0.678
LDL (mg/dL)	108.5±21.8	131.8±39.4	120.1±29.3	133.8±31.7	0.3889	0.5979
HDL (mg/dL)	55.0±13.4	51.3±12.3	41.0±8.1*	44.4±17.1	0.1776	0.5326
Total Cholesterol (mg/dL)	169.8±16.4	202.1±32.8*	181.7±34.9	197.6±41.9	0.2217	0.3169

Data (fasting values) are presented as mean ± SD, * p<0.05 vs lean controls

Table S1 Fibrosis and metabolic features.

	CT vs F01	CT vs F2	CT vs F34	F01 vs F2	F01 vs F34	F2 vs F34	Multivariate Analysis
FFA (mmol/l)	NS	NS	0.043	NS	NS	0.018	NS
SFA/UFA in FFA	0.015	0.0021	0.0044	NS	NS	NS	0.027
DNL index	0.033	0.0014	0.0009	NS	0.028	NS	0.0035
Adiponectin	0.0016	0.0009	0.043	NS	NS	NS	NS
TG (mmol/l)	0.0030	0.0233	0.0077	NS	NS	NS	NS
SFA/UFA in TG	NS	NS	0.006	NS	0.048	NS	NS
Insulin (mU/L)	0.0038	0.0002	0.0004	NS	0.0302	NS	0.030
EGP (μmol/min kg_FFM)	0.035	NS	0.0003	NS	0.048	0.043	0.05
Lipolysis (μmol/min)	0.030	0.0008	0.006	NS	NS	NS	NS
HOMA (mmol/l x mU/l)	0.005	0.0002	<0.0001	NS	0.042	NS	0.024
ADIPO-IR (mmol/l x mU/l)	NS	0.0545	<0.0001	NS	0.0031	0.043	0.05
Hep IR (μmol / (min*kg_FFM) x mU/l)	0.0038	<0.0001	<0.0001	NS	0.042	NS	0.012
Lipo IR (μmol/min x mU/l)	0.013	0.0005	0.0001	NS	NS	NS	NS
Muscle IR (mU/l / (ml/(min*kg_FFM))	NS	0.036	0.0062	NS	NS	NS	NS

SFA/UFA saturated to unsaturated fatty acid ratio; DNL: de novo lipogenesis index =palmitic/linoleic acid ratio; TG: triglycerides; EGP: endogenous glucose production; Mann-Whitney's test significant p-values for pairwise comparison among controls and subjects with NAFLD with different stages of fibrosis. In the last column, significant p-values for the independent contribution of fibrosis stage in a multivariate analysis (adjusted by IHTG) are reported.
NS: p values >0.05.

Figure 1

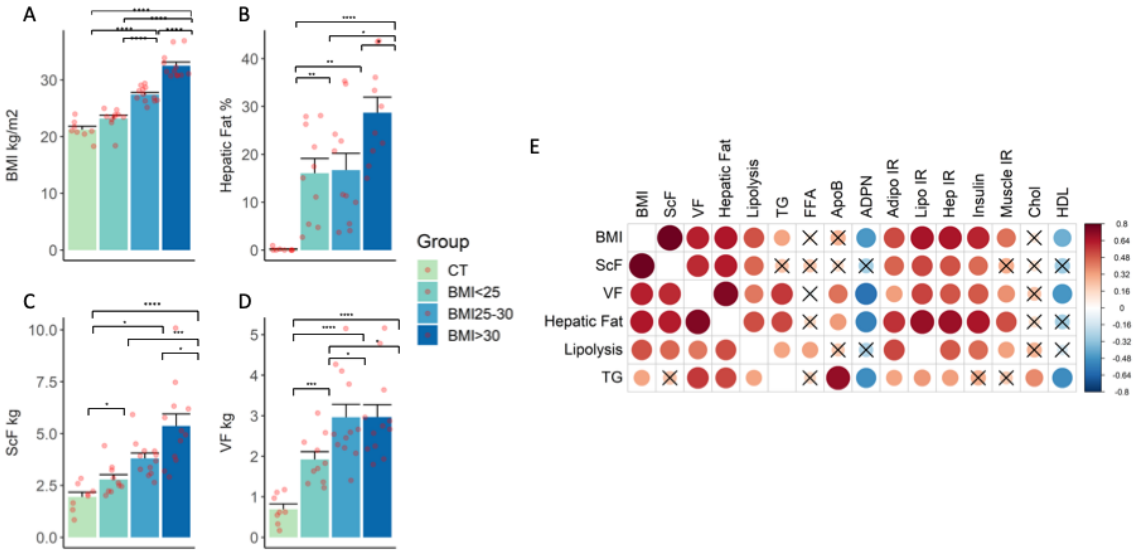

Figure 1. BMI (panel A) and intra hepatic triglyceride content measured by MRI, i.e., IHTG (panel B), subcutaneous fat (panel C), and visceral fat (panel D), in healthy controls and NAFLD subjects divided in accordance with their BMI (from light green to dark blue). Data are expressed as means ± SE, differences among the groups were tested using non-parametric Mann Whitney's test. Specific p values: *<0.05, ** <0.01, ***<0.001, ****<0.0001. Panel E shows the univariate correlation matrix between BMI, fat distribution, lipolysis and circulating TG and metabolic parameters in the entire cohort. Correlations that are not statistically significant (Pearson's p-value≥0.05) were crossed out.

Figure 2

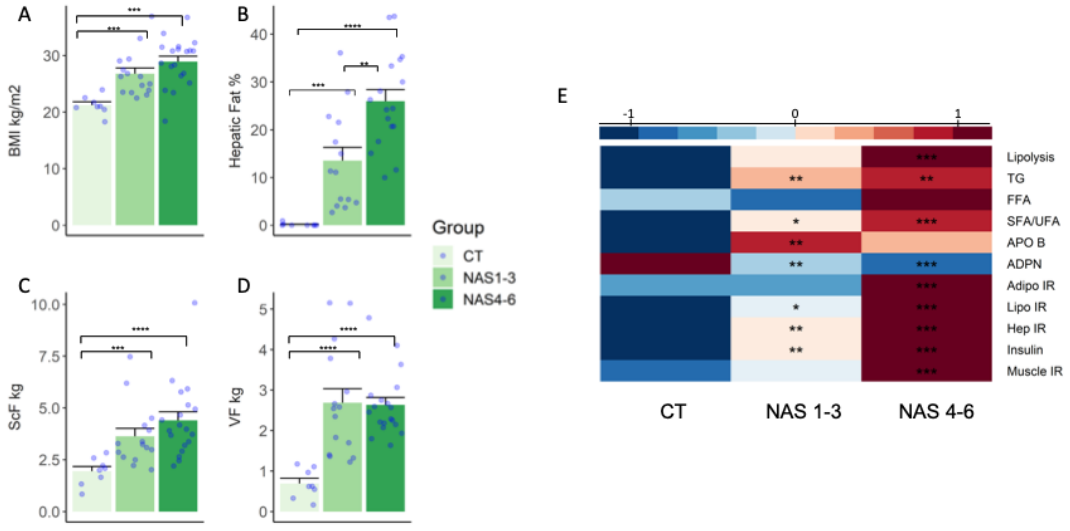

Figure 2. BMI (panel A) and fat distribution measured by MRI, i.e., IHTG (panel B), subcutaneous fat (panel C), visceral fat (panel D), in healthy controls and NAFLD subjects divided in accordance with their grade of steatosis, lobular inflammation and hepatocellular ballooning (NAS score), CT light green, NAS 1-3 and NAD 4-6 darker green (no subject had a NAS 7 or 8). Data are expressed as means ± SE, non-parametric Mann Whitney's test was used to test differences among the groups. Specific p values: *<0.05, ** <0.01, ***<0.001, ****<0.0001. In panel E heatmap of metabolic parameters were reported in controls and NAFLD subjects divided by their grade of NAS score. Values are reported as median within the groups and normalization was applied to the rows. Specific p values for non-parametric Mann Whitney's test vs control subjects: *<0.05, ** <0.01, ***<0.001, ****<0.0001.

Figure 3

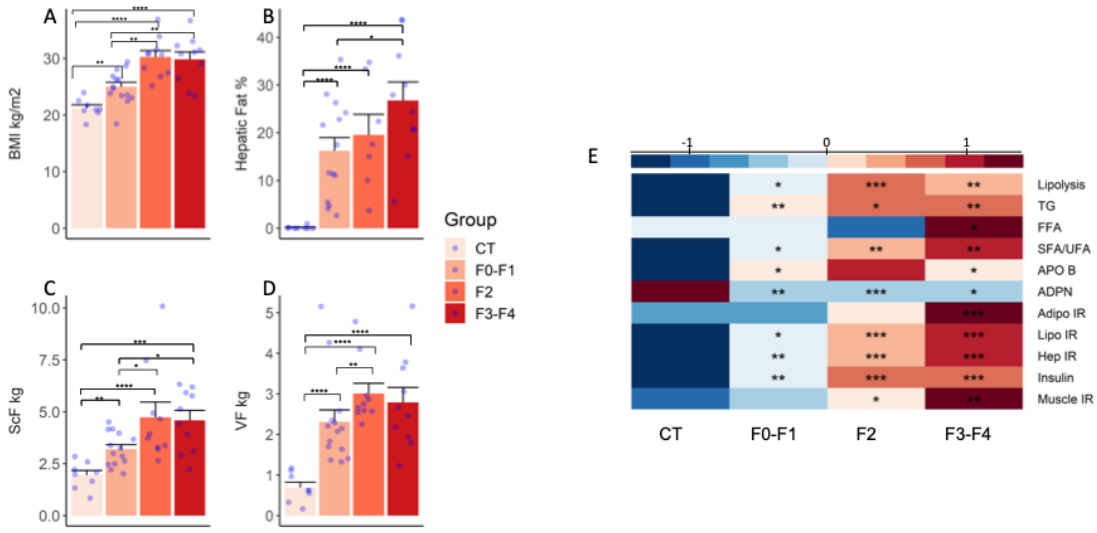

Figure 3. BMI (panel A) and fat distribution measured by MRI, i.e., IHTG (panel B), subcutaneous fat (panel C), visceral fat (panel D), in healthy controls and NAFLD subjects divided in accordance with their degree of fibrosis (CT pink, F0-1, F2 and F3-4 from red to dark red). Data are expressed as means ± SE, non-parametric Mann Whitney's test was used. Specific p values: *<0.05, ** <0.01, ***<0.001, ****<0.0001. In panel E heatmap of metabolic parameters were reported in controls and NAFLD subjects divided by their degree of fibrosis. Values are reported as median within the groups and normalization was applied to the rows. Specific p values for non-parametric Mann Whitney's test vs control subjects: *<0.05, ** <0.01, ***<0.001, ****<0.0001.

Figure 4

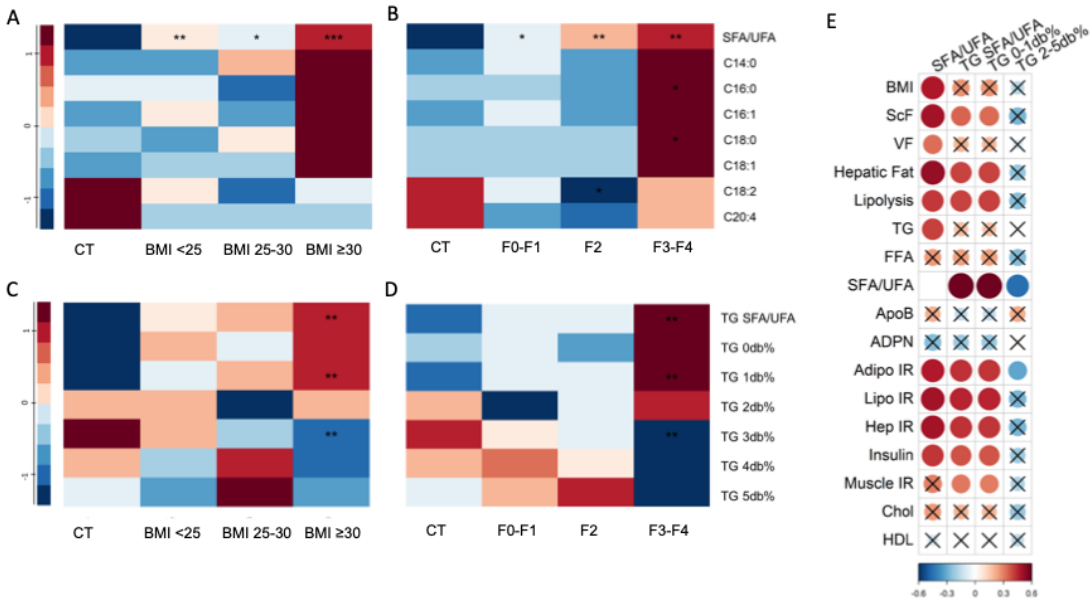

Figure 4. In panel A and B heatmaps of circulating FFA concentration levels and ratio of saturated to unsaturated FFA (SFA/UFA) in controls and NAFLD subjects divided by their BMI or degree of fibrosis, respectively. In panel C and D heatmaps of circulating TGs grouped in accordance with the numbers of double bonds and saturated to unsaturated TAG ratio in controls and NAFLD subjects divided by their BMI or degree of fibrosis, respectively. Values are reported as median within the groups, and normalization was applied to the rows. Specific p values for non-parametric Mann Whitney's test vs control subjects: *<0.05, ** <0.01, ***<0.001, ****<0.0001. In panel E Pearson's correlation matrix shows univariate association among the degree of saturation of FFA and TAG and metabolic parameters. Correlations that are not statistically significant (Pearson's p-value ≥ 0.05) were crossed out.

Supplementary Figure 1

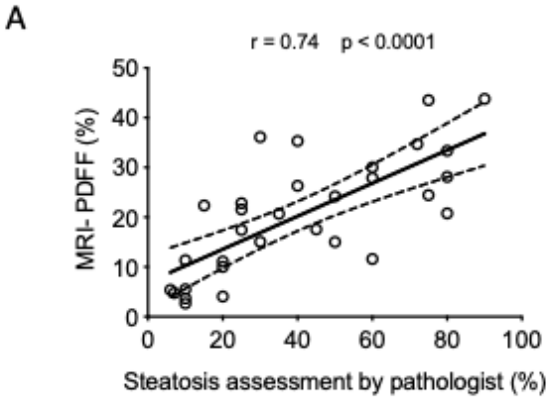

Supplementary figure 1. Linear correlation (panel A) between liver fat % assessed by the pathologist and hepatic fat % quantified by MRI PDFF; r = 0.74, p < 0.0001.

Supplementary Figure 2

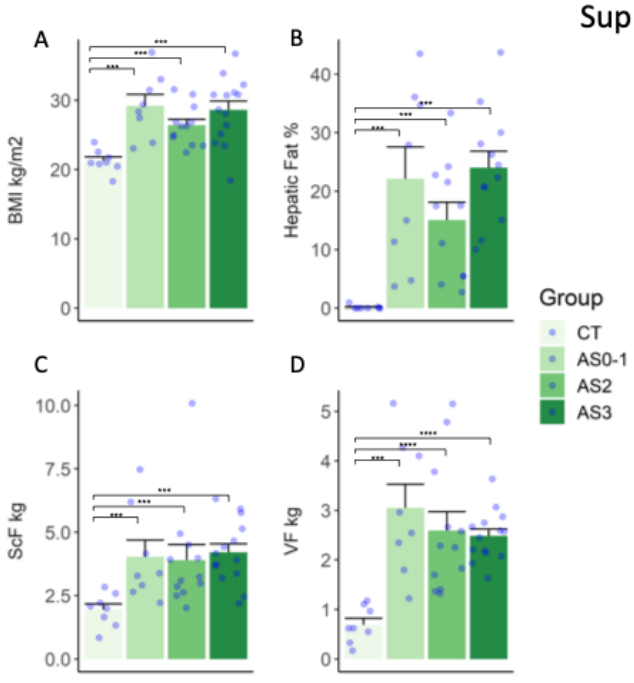

Supplementary figure 2. (A) BMI and fat distribution measured by MRI, i.e. IHTG (B), subcutaneous fat (C), visceral fat (D), in healthy controls and NAFLD subjects divided in accordance with their grade of lobular inflammation and hepatocellular ballooning (AS score) (from light green to dark green). Data are expressed as means ± s.e.m., non-parametric Mann Whitney's test was used to test differences among the group. Specific p values: *<0.05, ** <0.01, ***<0.001, ****<0.0001.